I&EC research
Industrial & Engineering Chemistry Research

ARTICLE

pubs.acs.org/IECR

Effect of Sulfur Poisoning in High Pressure Catalytic Partial Oxidation of Methane over Rh−Ce/Al_2O_3 Catalyst

Jin Ki Hong, Lingzhi Zhang,* Mark Thompson, Wei Wei, and Ke Liu

Fuel Conversion Laboratory, General Electric Global Research, 18A Mason, Irvine, California, 92618, United States

ABSTRACT: Short contact time catalytic partial oxidation (CPO) of methane has received increasing attention in industrial applications. Understanding of the catalytic system under high pressure and in the presence of sulfur represents a key challenge of this technology. This paper discusses CPO performance using a Rh−Ce catalyst supported on washcoat alumina foam under industrial relevant operating conditions (pressure up to 160 psig and different sulfur levels up to 16 ppm in methane). A long-term experimental run cycling between sulfur-free and sulfur injection conditions was conducted to examine the influence of sulfur on the catalyst. Sulfur effects were also evaluated under different sulfur levels and with different feed compositions. A dual zone reaction model was used to explain the effects of pressure, sulfur level, and the O/C ratio on CPO catalytic performance. Engineering challenges and requirements of the CPO process for industrial applications were discussed on the basis of recent advances in the understanding of CPO chemistry.

1. INTRODUCTION

Short contact time catalytic partial oxidation (CPO) technology has been successful for the conversion of gaseous fuels into synthesis gas (H_2 and CO).[1−9] The process occurs readily over group VIII noble metal catalysts, particularly Rh or Pt, supported on ceramic monolith or foam structures. The short contact time in the CPO process (milliseconds versus a few seconds for conventional steam reforming) enables the design of compact reactors for fuel conversion. Also, the selectivity of CPO toward syngas production can be greater than 90% depending on operating conditions. On the basis of fast kinetics and acceptable syngas selectivity, CPO has emerged as a suitable reaction path for onboard reforming of gaseous or liquid fuels for automotive and residential fuel cell systems and has been explored for industrial syngas production from natural gas for Fischer−Tropsch process or high value chemicals synthesis.[10−14] Further, the beneficial role of H_2 in fuel combustion leads to increased opportunity for CPO in industrial power generation technology.[15−18]

The CPO reaction route inside the catalyst bed has been intensively studied over many years. Two primary reaction routes have been proposed for the CPO of hydrocarbons, in particular, CH_4. Initially, it was thought that the hydrocarbon was converted in a "direct reaction route", similar to steam reforming, whereby hydrocarbon fuel adsorbs on the catalyst surface and pyrolyzes into adsorbed C and H atoms that then recombine with adsorbed O atoms to form a combination of H_2, H_2O, CO, and CO_2, depending on the fuel−air stoichiometry.[1,19,20] The general reaction equation that describes the direct route of CPO, including syngas generation along with H_2O and CO_2 in product stream, is as follows.[21]

$$CH_4 + (2 - x/2 - y/2)O_2 \rightarrow xH_2 + yCO + (2 - x)H_2O + (1 - y)CO_2 \quad (1)$$

More recently, an indirect reaction route has been proposed on the basis of experimental measurements of temperature and composition profiles across the reaction zones of a fixed bed monolithic reactor.[22] The indirect route proposes a two-zone model, where a strongly exothermic CH_4 combustion to H_2O and CO_2 dominates (eq 2) in the front zone of the catalyst and is subsequently followed by an endothermic steam and/or CO_2 reforming (eqs 3 and 4) of the remaining reacting fuel.

$$CH_4 + 2O_2 \rightarrow CO_2 + 2H_2O, \Delta H_r^\circ = -803\ \text{kJ/mol} \quad (2)$$

$$CH_4 + H_2O \rightarrow CO + 3H_2, \Delta H_r^\circ = +206\ \text{kJ/mol} \quad (3)$$

$$CH_4 + CO_2 \rightarrow 2CO + 2H_2, \Delta H_r^\circ = +247\ \text{kJ/mol} \quad (4)$$

It is highly probable that syngas produced may undergo a water gas shift (WGS) reaction (eq 5), and the H_2/CO ratio of syngas is adjusted in the rear section of the catalyst bed.

$$CO + H_2O \rightarrow CO_2 + H_2, \Delta H_r^\circ = -41\ \text{kJ/mol} \quad (5)$$

Recently, a method was developed that can measure temperature and species concentration profiles in situ inside a CPO catalyst bed (Rh or Pt supported on alumina foam) in a differential manner over a wide range of conditions. The method employs a movable direct-sampling capillary that is connected to a mass spectrometer for compositional analysis.[21,23−26] The CPO chemistry measured in situ indicates that O_2 is rapidly depleted, and a significant portion of CH_4 as reacting fuel is consumed to produce a mixture of H_2, H_2O, CO, and CO_2 within a short front section of the catalyst bed (oxidation zone). The near-complete oxygen depletion within the oxidation zone is accompanied by a steep temperature rise. Peak gas-phase temperature is observed when O_2 is depleted at the end of the oxidation zone, which is less than 3 mm away from the front end of the catalyst. In the remaining section, the combined measurement of temperature and species concentration indicates that

Received: October 25, 2010
Accepted: February 23, 2011
Revised: February 13, 2011
Published: March 09, 2011

syngas production occurs mainly through steam reforming routes of the remaining CH_4 fuel, and the WGS reaction occurs at comparable rates depending on H_2O and CO_2 enrichment.

Although CPO activity has been promising from lab-scale experiments, its application in industrial processes still requires further development to identify and mitigate potential technical risks in a number of aspects. So far, the comprehensive studies in CPO, performed mainly by academia, have been focused on understanding CPO activity over a wide spectrum of test conditions and CPO reaction routes on a variety of fuels ranging from CH_4, alcohols, bioderived liquids, and high carbon number liquid hydrocarbons to wood particles. From an industry point of view, the CPO process needs to be explored in more industrial process-related environments, including pressurized operation and its compatibility with impurities tolerance, including sulfur species in process fuel stream. Conventionally, chemical process design requires high pressure for increased process throughputs, overall process efficiency, and smaller equipment size. For example, the Fischer−Tropsch synthesis process normally requires downstream reactor pressure in excess of 500 psi and would even reach 1000 psi or higher in some cases,[27] requiring elevated pressure CPO reactor design and operation. From a fuel quality point of view, the tolerance of the CPO process to impurities present in the fuel stream is viewed as another developmental area that is highly important to industrial application.

This study is intended to experimentally investigate the sulfur impact on CPO activity under elevated pressure to bridge the gap between fundamental studies and industrial requirements. The experimental measurements of CPO under different feed O_2/C ratios and sulfur levels in the reacting fuel are presented. The effect of pressure, feed O_2/C ratios, and sulfur levels is discussed in terms of sulfur poisoning routes within the context of the CPO reaction mechanism discussed above. The CPO data gathered are analyzed in terms of methane conversion and H_2 and CO selectivities. CPO runs with sulfur-bearing fuel, including steady-state operation and startup/shutdown, is also presented herein.

2. EXPERIMENTAL SECTION

2.1. Catalyst Preparation. α-Alumina foams of 99.5% purity purchased from Vesuvius High-Tech Ceramics were used as CPO catalyst support. The support has a porous structure of 80 pores per inch, and its dimension is 20 mm in diameter and 20 mm in length. The washcoat was applied as γ-alumina onto the substrate to increase surface area and catalyst dispersion. The washcoated foam was calcined in air at 600 °C, and a washcoat loading of 3% by weight was obtained. The internal void fraction of the foam was experimentally determined by measuring the catalyst bed filling density and density of the foam. A diluted mixture of a precursor solution of $Rh(NO_3)_3$ (Alfa Aesar) and $Ce(NO_3)_3 \cdot 6H_2O$ (Alfa Aesar) was prepared for catalyst impregnation over the foam to achieve targeted catalyst loading. Half of the solution was impregnated on one face of the catalyst, followed by drying at 80 °C in a vacuum furnace. The other half of the solution was impregnated from the other face of the foam and subsequently dried in the same manner. The catalyst was calcined at 600 °C for 6 h before testing.

2.2. Experimental Apparatus. A metallic tubular reactor of 22 mm inner diameter was built for high pressure CPO experiments. The reactor was made of inconel material to ensure safety under the estimated temperature and pressure conditions. Both ends of the reactor were welded to flanges that allow a gas-tight seal under rated temperature and pressures. The finished CPO catalyst was wrapped in Fiberfrax paper so that the paper can provide a tight seal between the inner wall and the catalyst inside the reactor tube, allowing minimized bypass of feed stream and good heat exchange with the furnace. The reactor tube was located inside a tubular furnace for controlled preheating of the feed stream. The position of the catalyst was adjusted to allow proper preheating, while avoiding precombustion of the reacting fuel in the feed stream. Blank alumina foam was placed 2.5 in. above the catalyst in order to serve as heat shield and to promote mixing of feed mixture. K-type thermocouples were installed 2.5 in. above the catalyst to measure preheating temperature of feed mixture. Another blank foam with a hole in the center was placed facing the bottom face of the catalyst to provide a secure position for a K-type thermocouple to measure catalyst backface temperature.

Controlled flow of CH_4, air, and N_2 was provided by mass flow controllers (Brooks, 5850 Series). Liquid water, using a high-pressure metering pump (Eldex, Optos Series), entered a muffle furnace through a coiled tubing for steam generation. The CPO product stream was cooled through a shell-tube type heat exchanger, and the condensed water was collected and discharged by a water knockout pot. A backpressure regulator (Tescom, 26-1700 Series) was installed downstream of the water knockout for a pressurized CPO run. All experimental measurements including temperature, pressure, and flow rates were measured using Labview data acquisition.

2.3. Sulfur Injection. Both naturally existing sulfur compounds in natural gas as well as sulfur compounds injected into a natural gas pipeline for leak detection were considered for sulfur injection tests. A mixture containing 100 ppm H_2S, 250 ppm dimethyl sulfide, and 250 ppm methyl mercaptan in balance N_2 was mixed into the CPO feed to simulate a natural gas that contains sulfur. It needs to be noted that sulfur concentrations (levels) specified are in reference to CH_4 concentrations, not the CPO feed mixture. Sulfur levels of 0, 4, 8, and 16 ppm were employed in this study.

2.4. Product Analysis and Activity Quantification. Product gas analysis was performed using Agilent Micro Gas Chromatography (GC). The GC was equipped with a thermal conductivity detector and two columns (Molecular Sieve and Plot Q) for quantitative analysis of H_2, O_2, N_2, CH_4, CO, CO_2, and C2 hydrocarbons. Gas sampling to GC occurred downstream of a backpressure regulator. Overall, the fraction of C2 hydrocarbons were extremely small, and therefore, they were not counted in determination of the CPO activity. The GC was calibrated using certified calibration gas mixtures. The chromatograms were used for determination of CH_4 conversion, selectivity toward H_2 and CO production, and overall carbon balance. The N_2 peak served as an internal reference in data processing. Throughout the experiments, carbon balance stayed within ±2%. In all CPO tests, O_2 conversion was 100%, and there was no O_2 slip observed in CPO product stream. Steady-state CPO activity was obtained after monitoring process temperature and pressure level stabilization for at least 30 min to ensure process stability. In this study, H_2 and CO product selectivity is determined as follows.

$$H_2\ \text{Selectivity} = \frac{\text{Number of moles of } H_2 \text{ produced}}{2 \times \text{Number of moles of } CH_4 \text{ converted}} \quad (6)$$

$$\text{CO Selectivity} = \frac{\text{Number of moles of CO produced}}{\text{Number of moles of } CH_4 \text{ converted}} \quad (7)$$

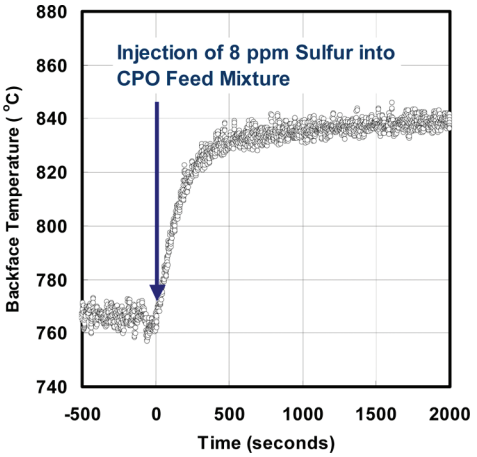

Figure 1. Catalyst backface temperature change during sulfur injection.

2.5. Equilibrium Calculation. Equilibrium compositions and CPO catalyst temperature under adiabatic conditions were determined using the AspenPlus process package. Feed mixture composition, preheating temperature, and reactor pressure were the required information for the calculation. The model employed for the equilibrium calculation was the RGibbs Reactor, and the reactor heat duty was set at zero for adiabatic condition of the reactor.

3. RESULTS

3.1. Reversibility of Sulfur-Induced Effect on CPO Activity. The effect of sulfur was investigated by injecting diluted sulfur compound mixture as described in section 2.3 into the CPO feed mixture of CH_4, air, and steam. Injection of sulfur compounds into the CPO feed mixture led to an instant rise in catalyst backface temperature and was accompanied by an increase in CH_4 slip in the CPO product stream, which corresponds to a reduced CH_4 conversion. The catalyst temperature rise measured upon sulfur compound injection in one set of tests is shown in Figure 1. The temperature rise was detected a few seconds after introducing a controlled flow of sulfur mixture into the CPO feed stream. The lead time observed for initiation of the temperature rise agreed roughly with the time estimated for the sulfur compound mixture to reach the CPO reactor, implying that the response of CPO activity to sulfur-containing compounds is instantaneous, within the scale of a few seconds. Catalyst temperature, as shown in Figure 1, rose rapidly during the first 500 s upon 8 ppm of sulfur injection to the CPO feed mixture and then slowed to approach an asymptotic value. Similarly, an instant drop in catalyst temperature was observed upon removal of sulfur from the feed stream during the first 500 s. The temperature then gradually approached an asymptotic value.

The effect of sulfur during a 300 h CPO test was investigated in order to understand the long-term sulfur effect on CPO activity (Figure 2). The test was conducted in three steps for gas cylinder management because of the large demand of gas supply for the reaction. Each 100 h run was started using a sulfur-free CPO feed mixture until steady state was obtained (approximately 3 h), and then the diluted sulfur compounds were injected for the remaining 97 h of the run. At the end of every 100 h run, sulfur injection was discontinued, and the CPO catalyst returned to a sulfur-free test condition before initiating the shutdown procedure. As shown in panel (a) of Figure 2, the catalyst backface

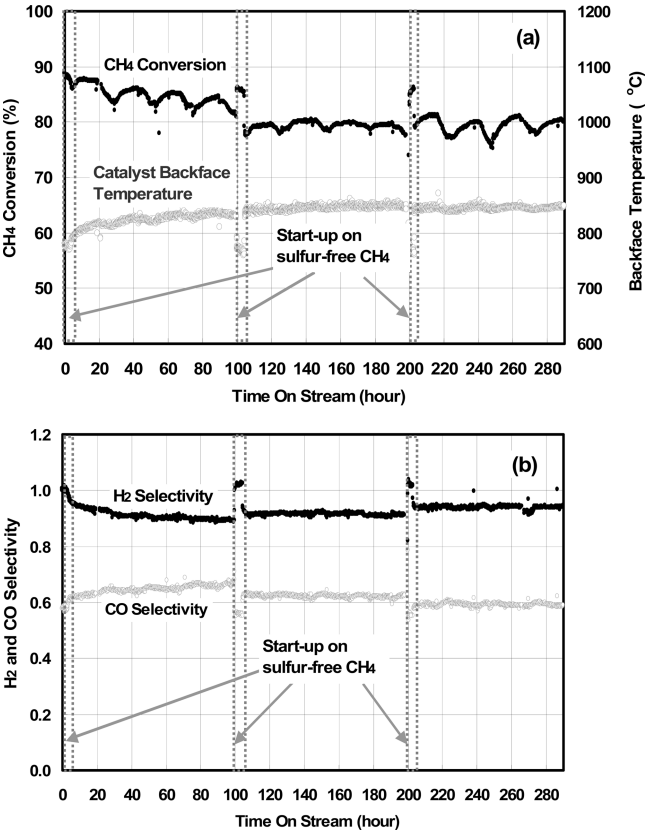

Figure 2. CPO measurement for 300 h of the run on CH_4 with 8 ppm sulfur (O_2/C = 0.67, H_2O/C = 1, preheating at 350 °C, 160 psi): (a) CH_4 conversion and catalyst backface temperature; (b) product selectivity.

temperature rose from approximately 780 °C to over 800 °C upon sulfur injection, and the increase continued gradually over the 100 h test period. CH_4 conversion showed a gradual drop from 89% upon sulfur injection and stabilized at 80% near the end of the 100 h test period. The change in both catalyst temperature and CH_4 conversion upon sulfur injection became more pronounced and reproducible as the test continued in the following 100 h of the test and afterward. CH_4 conversion stayed stable at 80%, and catalyst temperature also remained at 840 °C on the sulfur-injected feed mixture. The oscillating CH_4 conversion pattern that repeats every 24 h can be attributed to the daily change in the laboratory ambient temperature. The same pattern has also been observed in earlier studies for separate fuel processing experiments, and it was not considered as being representative of the characteristic of the CPO catalyst itself.

Panel (b) of Figure 2 shows the change in H_2 and CO selectivity upon sulfur injection. H_2 selectivity on the sulfur-free CPO feed mixture was measured to be 1, which corresponds to 2 mol of H_2 produced per mole of CH_4 converted. Upon sulfur injection, H_2 selectivity gradually dropped and stabilized at 0.9. In contrast, sulfur injection increased the CO selectivity slightly, and it was reproducible in the following 100 h run. It appears from panel (b) of Figure 2 that the changes in H_2 and CO selectivity caused by sulfur injection becomes less pronounced as the CPO run was repeated for the second and third run of 100 h of the test, even though CH_4 conversion and catalyst backface temperature showed highly pronounced and reproducible changes upon sulfur injection in the same test period. The less

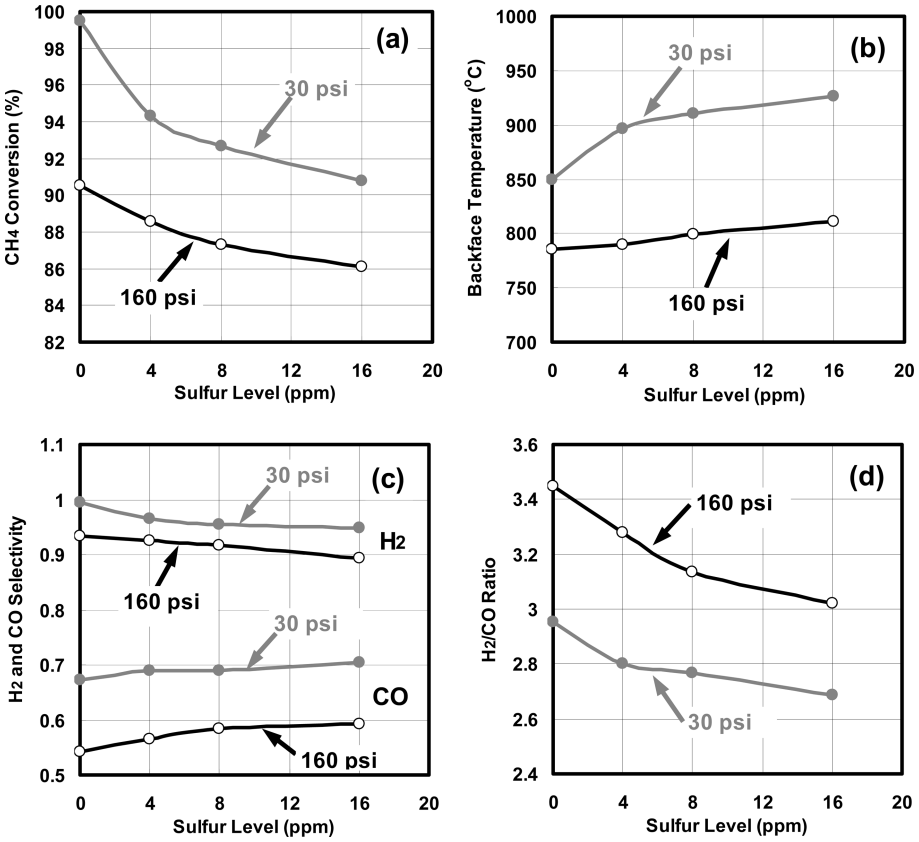

Figure 3. CPO measurement change on different sulfur injections (O_2/C = 0.67, H_2O/C = 1, preheating at 350 °C, pressure = 30 and 160 psi, respectively): (a) CH_4 conversion; (b) backface temperature; (c) H_2 and CO selectivity; and (d) H_2/CO ratio.

pronounced changes in both H_2 and CO selectivity observed over the extended run time as described above is difficult to quantify at this stage, as it might be related to the slow aging process of the catalyst.

3.2. CPO Measurements at Different Sulfur Levels. In this section, CPO activity was measured on different levels of sulfur (0, 4, 8, and 16 ppm) in the feed. It should be noted from observations in Figure 3 that changes in CPO activity including CH_4 conversion, H_2 and CO selectivity, and catalyst temperature are more pronounced as the catalyst is aged through repetition of extended CPO runs. Therefore, it should be noted that results obtained on a fresh CPO catalyst were slightly different than those obtained using an aged catalyst (e.g., ~88% CH_4 conversion at no sulfur and 160 psi in Figure 2 vs ~91% CH_4 conversion under the same condition in Figure 3).

The CPO activity change on different sulfur levels in the feed stream is shown in Figure 3. In panel (a) of Figure 3, CH_4 conversion of >99% was measured on a sulfur-free feed stream at 30 psi, and the conversion dropped to approximately 94% as sulfur content was increased to 4 ppm. Further increase in sulfur content to 8 ppm and 16 ppm led to rather gradual drop in CH_4 conversion. Increase in pressure to 160 psi from 30 psi reduced the CH_4 conversion. Sulfur-free CH_4 conversion was slightly above 90% at 160 psi. Sulfur injection led to a rather mild decrease in CH_4 conversion compared to 30 psi data, reaching 86% conversion at 16 ppm.

Panel (b) of Figure 3 compares the CPO catalyst backface temperature measured at different sulfur levels. At 30 psi, a catalyst temperature of 850 °C was measured on sulfur-free CH_4, and the temperature rose approximately 50 °C upon increase of sulfur level to 4 ppm. Further increase in the sulfur level to 16 ppm from 4 ppm led to a small increase in temperature. Catalyst temperature dropped as operation pressure was elevated to 160 psi. On sulfur-free CH_4, catalyst temperature measured was below 800 °C, which is approximately 70 °C lower than that of the 30 psi test. Catalyst temperature rose at 160 psi in the presence of sulfur, but the increase was not as pronounced as in the 30 psi test.

The H_2 and CO selectivity changes with sulfur level showed contrasting behaviors (Figure 3). The H_2 selectivity decreased with sulfur level at both pressures, while CO selectivity showed an increasing pattern with sulfur level. Both H_2 and CO selectivity dropped as the reactor pressure was elevated to 160 psi. The H_2/CO ratio in the CPO product stream, shown in panel (d) of Figure 3, decreased with sulfur level at both pressures, which can be ascribed to the reduced steam reforming activity when sulfur is present (see Results discussion). Steam reforming reaction produces more H_2 compared with the partial oxidation reaction. The ratio was higher on the 160 psi test, and it stayed above 3 on 16 ppm sulfur. For the 30 psi test, the ratio decreased to approximately 2.7 on 16 ppm sulfur.

3.3. Sulfur Poisoning Effect As a Function of O_2/C Ratios. To understand the potential influence of the O_2/C ratio on the sulfur poisoning effect, a new fresh catalyst was loaded into the reactor, and the performance was stabilized prior to data acquisition. It should be noted that a fresh catalyst was loaded for experiments in this section instead of using the aged catalyst in sections 3.1 or 3.2 to eliminate influence from catalyst aging.

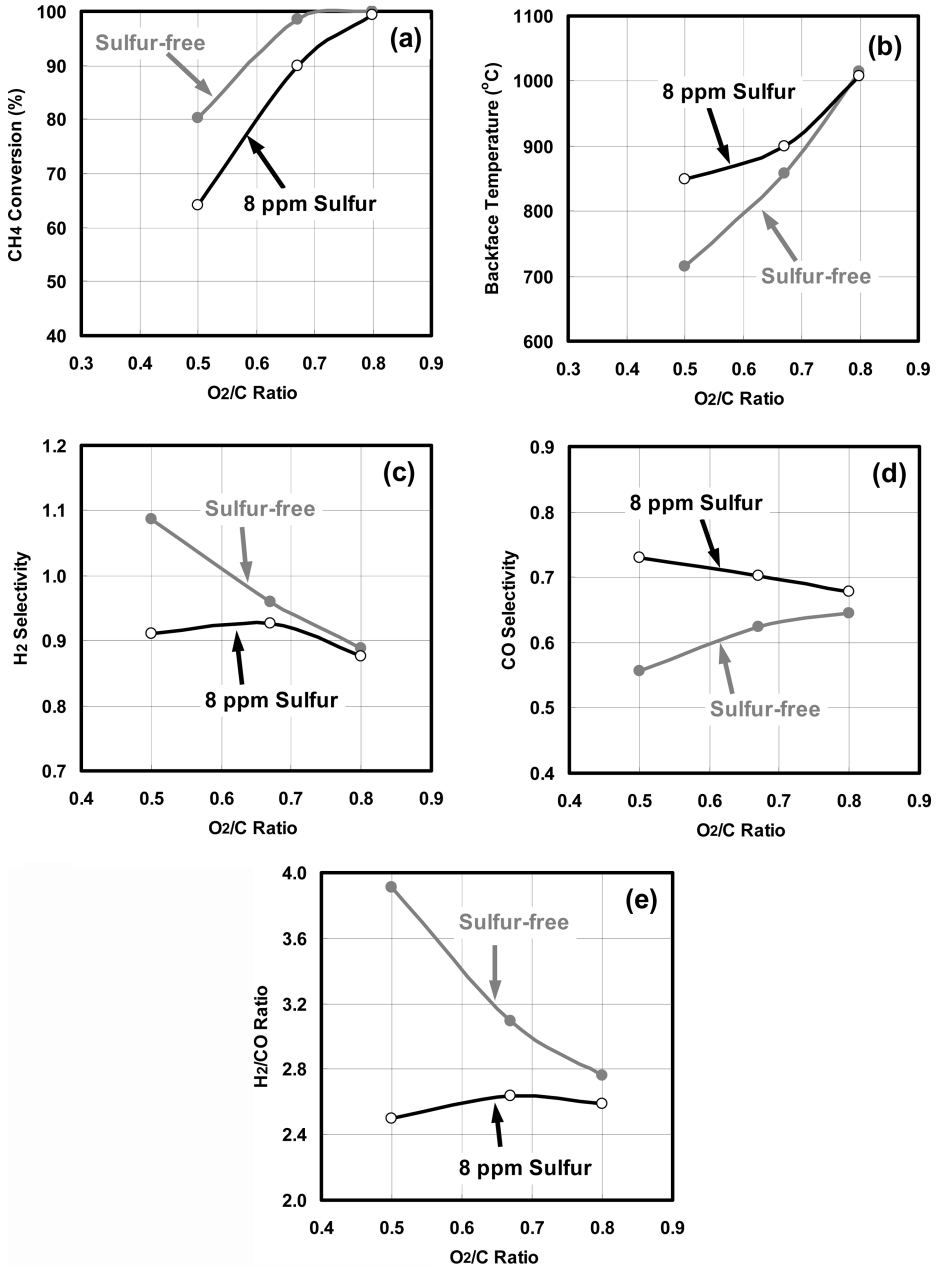

Figure 4. Effect of O_2/C ratio on CPO performance with 8 ppm sulfur in CH_4 (H_2O/C = 1, preheating at 350 °C, pressure = 30 psi): (a) CH_4 conversion; (b) backface temperature; (c) H_2 selectivity; (d) CO selectivity; (e) H_2/CO ratio.

Therefore, although some of the test conditions specified in this section may coincide with those of previous sections, the data obtained do not demonstrate perfect reproducibility. Figure 4 compares sulfur poisoning effects at three different O_2/C ratios. On the sulfur-free test, both CH_4 conversion and catalyst backface temperature rose with the O_2/C ratio, as expected from the increasing contribution of oxidation/combustion. It is evident from Figure 4 that the impact of sulfur on CPO became more pronounced at the lower O_2/C ratio. At an O_2/C ratio of 0.8, virtually no noticeable change in CH_4 conversion and backface temperature was observed upon 8 ppm sulfur injection. As the O_2/C ratio was reduced to 0.5, sulfur injection lowered CH_4 conversion by about 15%, and catalyst temperature rose by about 150 °C. During the 8 ppm sulfur test, the H_2 and CO selectivity and H_2/CO ratio remained relatively stable over the O_2/C ratios investigated, which is quite different from sulfur-free test. This contrasted with the sulfur-free CPO results in which the H_2 and CO selectivities changed substantially as the O_2/C ratio increased.

4. DISCUSSION

The CPO activity presented in the previous section is determined by multiple factors, including the inherent CPO mechanism, shift in thermodynamics upon pressurization, and kinetics inhibition by sulfur poisoning.

4.1. Effect of Pressure on CPO Activity. In the absence of sulfur, both the CH_4 conversion and catalyst temperature decreased significantly upon elevation of pressure (Figure 3).

dx.doi.org/10.1021/ie102159w |*Ind. Eng. Chem. Res.* 2011, 50, 4373–4380

Table 1. Thermodynamic Equilibrium Predicted on CPO Runs vs Experimental Measurements[a]

pressure (psi)	30			160		
heat loss (%)	0.0 (adiabatic)	Figure 3 data	1.7	0.0 (adiabatic)	Figure 3 data	5.9
backface temperature (°C)	905	851	851	912	785	785
CH_4 conversion (%)	100	99.5	99.9	99.3	90.5	92.2
H_2 selectivity	0.98	0.99	0.99	0.97	0.93	0.97
CO selectivity	0.71	0.67	0.68	0.71	0.54	0.60
H_2/CO ratio	2.77	2.96	2.91	2.75	3.45	3.25

[a] Heat removal was applied in the calculation in order to match the catalyst backface temperature measured in the CPO run.

Also, pressurization caused significant changes in H_2 and CO selectivity and the H_2/CO ratio. These results are compared in Table 1, with the values calculated from thermodynamic equilibrium assuming negligible heat loss from the CPO reactor to the environment (adiabatic operation). Thermodynamic prediction for adiabatic conditions shows no noticeable difference in CPO conversion, H_2 and CO selectivity, and H_2/CO ratio between the two pressure levels. Further, a slight increase in temperature is predicted, from 905 °C at 30 psi to 912 °C at 160 psi. This contrasts with the experimental results in which a significant drop in backface temperature was observed (912 to 785 °C). Thus, there appears to be a poor agreement between the results and the thermodynamic predictions for adiabatic conditions. Considering the low temperature (below 400 °C) preheating furnace that surrounds the CPO catalyst, heat loss from the CPO catalyst was considered to be a primary cause for the deviation. The heat loss during the experiment cannot be easily measured. To test this hypothesis, ASPEN runs with heat losses calculated from the RGibbs Reactor model were iterated until the predicted equilibrium temperature matched closely with measured CPO catalyst backface temperature shown in Table 1. The heat loss was estimated to be approximately 1.7% of the heating value of the CH_4 fuel at 30 psi and increased to 5.9% as pressure was elevated to 160 psi. Upon matching the catalyst temperature, the CPO activity prediction with heat loss considered agreed more closely with the experimental CPO data (Table 1) and, thus, explains the majority of the deviation of CPO measurements with equilibrium predictions for adiabatic conditions.

The increase in heat loss upon pressurization could be due to the combination of increased gas thermal conductivity and increased heat transfer at the gas/reactor interface. From dual reaction zone perspective of CPO, the increased residence time upon pressurization would be beneficial in terms of CH_4 conversion, particularly for the kinetically sluggish steam reforming occurring in the rear section of the catalyst bed. However, in this elevated pressure CPO run, the beneficial residence time effect upon pressurization is largely shadowed by increased heat loss.

4.2. Sulfur Poisoning. Over almost all experimental conditions, sulfur injection into the CPO feed stream caused an increase in backface temperature. As is evident from Figures 3 and 4, the level of temperature rise varied widely depending on pressure, sulfur injection level, and O_2/C ratio. A closer look at the data indicates that the level of temperature rise is shown to be roughly proportional to the change in CH_4 conversion over the whole test conditions. In Figure 3, a temperature rise from 785 to 811 °C at 160 psi upon increasing sulfur level from 0 to 16 ppm was accompanied by CH_4 conversion reduction from 90% to 86%. A more pronounced increase in temperature rise was accompanied by a larger decrease in CH_4 conversion at 30 psi. CPO data at different O_2/C ratios also exhibit the same trend. Negligible changes in both temperature and CH_4 conversion were observed upon 8 ppm sulfur injection at a O_2/C ratio of 0.8. When the O_2/C ratio was dropped to 0.5, a greater than 10% drop in CH_4 conversion was accompanied by a greater than 50 °C increase in catalyst temperature.

Recent studies employing a traversing probe for spatial profiling of species and temperature inside the CPO catalyst provided strong evidence that the CPO catalyst consists of multiple reaction zones in series.[21,23−26] The oxidation zone is the front section of the CPO catalyst where O_2 is rapidly consumed by reacting with part of CH_4 to produce H_2, H_2O, CO, and CO_2. A steep temperature gradient is established within this short oxidation zone as a result of a rapid consumption of O_2. The length of the oxidation zone, experimentally measured to be between 1−2 mm, was observed to be independent of the feed O_2/C ratios. Further analysis of the O_2 profile in the oxidation zone indicated that oxidation kinetics are fully under mass transport control.[21] The remaining CH_4 exiting the oxidation zone is gradually converted by steam reforming in the rest of the catalyst, as evidenced by a gradual growth of H_2 and CO signals accompanied by a corresponding drop in CH_4 and catalyst temperature. The observation of temperature rise and methane conversion drop upon sulfur injection, within the context of the above-discussed dual zone model, suggests that less heat is consumed in the reforming zone.

A recent study from professor Schmidt's group reported a CH_4 profile change in the reforming section by sulfur injection.[28] In the study, sulfur injection into the CPO feed stream inhibited steam reforming activity in the reforming zone, while both the CH_4 and O_2 profiles in the oxidation zone were seen to remain unchanged with sulfur levels up to 28 ppm CH_3SH. The profile result by CH_3SH injection is highly relevant to this study and explains the rise in temperature and drop in CH_4 conversion observed upon sulfur injection. The inhibition of highly endothermic steam reforming by sulfur compounds translates to both catalyst temperature and CH_4 conversion at the end of oxidation zone delivered all the way to the end of the CPO catalyst without experiencing a heat-consuming steam reforming reaction. Sulfur poisoning of the CPO reaction over the Rh monolith catalyst was claimed to be independent of sulfur-bearing compounds and only indirectly affected by the type of catalyst support through the value of Rh dispersion.[29] In this study, sulfur-bearing compounds employed include H_2S, dimethyl sulfide, and methyl mercaptan. In petroleum refineries, sulfur-bearing compounds are converted to H_2S through reaction with pressurized H_2 at 300−400 °C over Mo-based catalysts.[30] It is highly probable that the high temperature and reducing environment in this study would lead to near complete conversion of sulfur-bearing

compounds to H_2S within the oxidation zone of CPO. The near full coverage of the Rh catalyst by adsorbed oxygen coupled with the hot catalyst surface is considered to inhibit adsorption of sulfur in the oxidation zone.

In this study, pressure is not seen to be a major factor that contributes to catalyst sulfur poisoning. The only noticeable difference is that the initial activity loss when sulfur increased from 0 to 4 ppm is more pronounced at 30 psi in comparison with the trend at 160 psi (Figure 3). A previous study presented CPO kinetics information at elevated pressure.[25] Pressure variation between 0.1 and 1.1 MPa did not change either CH_4 or O_2 profiles over the Rh catalyst at constant mass flow rates, leading to the argument that CPO is under a mass transfer limitation under the elevated pressure conditions.

The reduced sulfur poisoning effect at higher O_2/C ratios (Figure 4) can be explained within the context of dual reaction zone model. With an increase in the O_2/C ratio of the CPO feed stream, CH_4 conversion through the oxidation zone increases and a smaller fraction of CH_4 enters the neighboring reforming zone for steam reforming. This translates to a reduced contribution of the steam reforming reaction to the overall CH_4 conversion through the CPO catalyst. Because the sulfur is observed to kinetically inhibit just the steam reforming reaction, a reduced contribution of steam reforming at high O_2/C ratios would mean that the drop in CH_4 conversion upon sulfur injection would become less pronounced. At low O_2/C ratios, the reverse is true. The CH_4 conversion in the oxidation zone would decrease accordingly, leaving more CH_4 available for steam reforming in the reforming zone. The increased contribution of steam reforming would lead to a more pronounced drop in CH_4 conversion upon sulfur injection.

The catalyst temperature may also affect the magnitude of the sulfur poisoning effect. Sulfur poisoning of the CPO catalyst, incurred by adsorption of H_2S and impacting the steam reforming through either steric effect or ensemble effect, is highly dependent on catalyst temperature, more specifically surface mobility.[28] At the higher temperatures observed at high O_2/C ratios, the kinetic inhibition of the steam reforming reaction could be reduced leading to a less pronounced sulfur poisoning effect in overall CH_4 conversion.

In summary, the catalyst temperature and amount of CH_4 available for steam reforming, depending on the CPO feed O_2/C ratio, are considered to contribute to the overall CH_4 conversion reduction upon sulfur injection. A more quantitative analysis of the sulfur poisoning effect would involve detailed kinetics of steam reforming and sulfur-induced steam reforming kinetics changes.

4.3. CPO in Industrial Application. CPO-to-syngas operating on pipeline natural gas at pressure has the potential in industrial applications for gas-to-liquid or high-value chemical synthesis. This study presents a clear picture on the prediction of syngas composition (H_2/CO ratio) and catalyst temperatures with varying feed mixtures and on the understanding of heat loss at elevated pressure. Experimental findings from this work guides reactor design, operating conditions selection, and catalyst specification at large scales. However, more work needs to be conducted before the technology is ready for commercialization. Although CPO performance over a 300 h period has been demonstrated (Figure 2) in this work, long-term process durability needs to be guaranteed. The scope of sulfur poisoning may need to include startup and shutdown transient dynamics besides steady-state runs. To allow fuel flexibility of the CPO application, more hydrocarbon fuels need to be examined using this technology, such as long chain hydrocarbons, diesel, alcohols, etc.

5. CONCLUSIONS

The poisoning effect of sulfur in methane CPO was studied under elevated reactor pressure up to 160 psi. The Rh−Ce supported foam catalyst demonstrated stable long-term performance with 8 ppm sulfur in the natural gas stream. It was found that the sulfur did not cause a permanent poisoning effect on the catalyst under our operating conditions. Catalyst performance (methane conversion, product selectivities, catalyst backface temperature, etc.) can be recovered when sulfur is removed from the stream. Sulfur injection up to 16 ppm led to a drop in methane conversion and the H_2/CO ratio in the CPO product stream, while increasing catalyst backface temperature. The sulfur poisoning effect was more pronounced as the O_2/C ratio was decreased. A recently established CPO dual reaction zone model was used to explain the sulfur poisoning effect. Another finding is that under small-scale setup, elevation of the CPO reactor pressure resulted in reduced methane conversion and catalyst temperature through increased heat loss to the environment, which may be an important consideration in process scaleup.

AUTHOR INFORMATION

Corresponding Author

*E-mail: zhanglin@ge.com. Phone: 949-330-8113. Fax: 949-330-8994.

ACKNOWLEDGMENT

This work was supported by the DOE Grant DE-FG36-05GO15023 and was performed in collaboration with Professor Lanny Schmidt at the University of Minnesota and Dr. Ted Krause at the Argonne National Laboratory. Their helpful comments are gratefully acknowledged.

REFERENCES

(1) Hickman, D. A.; Schmidt, L. D. Synthesis gas formation by direct oxidation of methane over Pt monoliths. *J. Catal.* **1992**, *138*, 267.

(2) Hickman, D. A.; Haupfear, E. A.; Schmidt, L. D. Synthesis gas formation by direct oxidation of methane over Rh monoliths. *Catal. Lett.* **1993**, *17*, 223.

(3) Huff, M.; Schmidt, L. D. Production of olefins by oxidative dehydrogenation of propane and butane over monoliths at short contact times. *J. Catal.* **1994**, *149*, 127.

(4) Huff, M.; Schmidt, L. D. Oxidative dehydrogenation of isobutane over monoliths at short contact times. *J. Catal.* **1995**, *155*, 82.

(5) Witt, P. M.; Schmidt, L. D. Effect of flow rate on the partial oxidation of methane and ethane. *J. Catal.* **1996**, *163*, 465.

(6) Tanaka, H.; Kaino, R.; Nakagawa, Y.; Tomishige, K. Comparative study of Rh/MgO modified with Fe, Co or Ni for the catalytic partial oxidation of methane at short contact time. Part II: Catalytic performance and bed temperature profile. *Appl. Catal., A* **2010**, *378*, 187.

(7) Tanaka, H.; Kaino, R.; Okumura, K.; Kizuka, T.; Tomishige, K. Catalytic performance and characterization of Rh-CeO_2/MgO catalysts for the catalytic partial oxidation of methane at short contact time. *J. Catal.* **2009**, *268*, 1.

(8) Nogare, D. D.; Degenstein, N. J.; Horn, R.; Canu, P.; Schmidt, L. D. Modeling spatially resolved data of methane catalytic partial oxidation on Rh Foam Catalyst at different inlet compositions and flowrates. *J. Catal.* **2011**, *277*, 134.

(9) Basile, F.; Benito, P.; Fornasari, G.; Monti, M.; Scavetta, E.; Tonelli, D.; Vaccari, A. Novel Rh-based structured catalysts for the catalytic partial oxidation of methane. *Catal. Today* **2010**, *157*, 183.

(10) Wright, H. A.; Allison, J. D.; Jack, D. S.; Lewis, G. H.; Landis, S. R. ConocoPhillips GTL technology: The COPox™ process

as the SynGas generator. *Am. Chem. Soc., Div. Fuel Chem.* **2003**, *48* (2), 791.

(11) Farrauto, R.; Hwang, S.; Shore, L.; Ruettinger, W.; Lampert, J.; Giroux, T.; Liu, Y.; Ilinich, O. New material needs for hydrocarbon fuel processing: Generating hydrogen for the PEM fuel cell. *Ann. Rev. Mater. Res.* **2003**, *33*, 1.

(12) Kang, I.; Bae, J.; Bae, G. Performance comparison of autothermal reforming for liquid hydrocarbons, gasoline and diesel for fuel cell applications. *J. Power Sources* **2006**, *163*, 538.

(13) Kang, I.; Bae, J.; Yoon, S.; Yoo, Y. Performance improvement of diesel autothermal reformer by applying ultrasonic injector for effective fuel delivery. *J. Power Sources* **2007**, *172*, 845.

(14) Chaniotis, A. K.; Poulikakos, D. Modeling and optimization of catalytic partial oxidation methane reforming for fuel cells. *J. Power Sources* **2005**, *142*, 184.

(15) Boschek, E.; Griebel, P.; Erne, D.; Jansohn, P. In Lean Blowout Limits and NO*x* Emissions of Turbulent, Lean Permixed, High Pressure CH_4/H_2/Air Flames, 8th International Conference on Energy for a Clean Environment: Clean Air 2005, Lisbon, Portugal, 2005, pp 1−12.

(16) Dunstan, T. D.; Jenkins, K. W. The effects of hydrogen substitution on turbulent premixed methane−air kernels using direct numerical simulation. *Int. J. Hydrogen Energy* **2009**, *34*, 8389.

(17) Schefer, R. W. Hydrogen enrichment for improved lean flame stability. *Int. J. Hydrogen Energy* **2003**, *28*, 1131.

(18) TerMaath, C. Y.; Skolnik, E. G.; Schefer, R. W.; Keller, J. O. Emissions Reduction benefits from hydrogn addition to midsize gas turbine feedstocks. *Int. J. Hydrogen Energy* **2006**, *31*, 1147.

(19) Schmidt, L. D.; Huff, M. Partial oxidation of CH_4 and C_2H_6 over noble metal coated monoliths. *Catal. Today* **1994**, *21*.

(20) Zerkle, D. K.; Allendorf, M. D.; Wolf, M.; Deutschmann, O. Understanding homogeneous and heterogeneous contributions to the platinum-catalyzed partial oxidation of ethane in a short-contact-time reactor. *J. Catal.* **2000**, *196*, 18.

(21) Horn, R.; Williams, K. A.; Degenstein, N. J.; Bitsch-Larsen, A.; Dalle Nogare, D.; Tupy, S. A.; Schmidt, L. D. Methane catalytic partial oxidation on autothermal rh and pt foam catalysts: oxidation and reforming zones, transport effects, and approach to thermodynamic equilibrium. *J. Catal.* **2007**, *249*, 380.

(22) Heitnes, K.; Lindberg, S.; Rokstad, O. A.; Holmen, A. Catalytic partial oxidation of methane to synthesis gas. *Catal. Today* **1995**, *24*, 211.

(23) Panuccio, G. J.; Schmidt, L. D. Species and temperature profiles in a differential sphere bed reactor for the catalytic partial oxidation of *n*-octane. *Appl. Catal., A* **2007**, *332*, 171.

(24) Horn, R.; Williams, K. A.; Degenstein, N. J.; Schmidt, L. D. Syngas by catalytic partial oxidation of methane on rhodium: mechanistic conclusions from spatially resolved measurements and numerical simulations. *J. Catal.* **2006**, *242*, 92.

(25) Bitsch-Larsen, A.; Horn, R.; Schmidt, L. D. Catalytic partial oxidation of methane on rhodium and platinum: Spatial profiles at elevated pressure. *Appl. Catal., A* **2008**, *348*, 165.

(26) Michael, B. C.; Donazzi, A.; Schmidt, L. D. Effects of H_2O and CO_2 addition in catalytic partial oxidation of methane on Rh. *J. Catal.* **2009**, *265*, 117.

(27) Elbashir, N. O.; Bao, B.; El-Halwagi, M. An Approach to the Design of Advanced Fischer−Tropsch Reactor for Operation in Near-Critical and Supercritical Phase Media. In Proceedings of the 1st Annual Gas Process Symposium; Elsevier: Amsterdam, 2009.

(28) Bitsch-Larsen, A.; Degenstein, N. J.; Schmidt, L. D. Effect of Sulfur in Catalytic Partial Oxidation of Methane over Rh-Ce Coated Foam Monoliths. *Appl. Catal., B* **2008**, *78*, 364.

(29) Cimino, S.; Torbati, R.; Lisi, L.; Russo, G. Sulphur inhibition on the catalytic partial oxidation of methane over Rh-based monolith catalysts. *Appl. Catal., A* **2009**, *360*, 43.

(30) Satterfield, C. N. *Heterogeneous Catalysis in Practice*; McGraw-Hills Book Company: New York, 1980.

(31) Wang, L.; Murata, K.; Inaba, M. Development of novel highly active and sulphur-tolerant catalysts for steam reforming of liquid hydrocarbons to produce hydrogen. *Appl. Catal., A* **2004**, *257*, 43.